Optimizing PECVD a-SiC:H Films for Neural Interface Passivation

Scott Greenhorn, Konstantinos Zekentes, Edwige Bano, Valerie Stambouli, Andrei Uvarov

Key Engineering Materials
ISSN: 1662-9795, Vol. 947, pp 83-88
doi:10.4028/p-762f40

Submitted: 2022-09-03
Revised: 2023-01-06
Accepted: 2023-01-09
Online: 2023-05-31

Optimizing PECVD a-SiC:H Films for Neural Interface Passivation

Scott Greenhorn[1,2,3,a*], Konstantinos Zekentes[2,3,b], Edwige Bano[2,c], Valérie Stambouli[1,d], and Andrei Uvarov[4,e]

[1]Laboratoire des Matériaux et de la Génie Physique, Grenoble INP, France

[2]Institut de Microélectronique Electromagnétisme et Photonique et le Laboratoire d'Hyperfréquences et de Caractérisation, Grenoble INP, France

[3]Foundation for Research and Technology – Hellas, Greece

[4]Plasma-therm Europe, France

[a*]scott.greenhorn@grenoble-inp.fr, [b]trifili@physics.uoc.gr, [c]edwige.bano@grenoble-inp.fr, [d]Valerie.Stambouli-Sene@grenoble-inp.fr, [e]Andrei.Uvarov@corial.com

Keywords: Neural Interface, Biosensor, PECVD, Amorphous

Abstract. This work aims to optimize Plasma-Enhanced Chemical Vapour Deposition (PECVD) amorphous hydrogenated silicon carbide (a-SiC:H) as a conformal passivation layer for invasive microelectrode array (MEA) neural interface applications. By carefully tuning the PECVD deposition parameters, the composition, structure, electrical, and mechanical properties of the films can be optimized for high resistivity, low stress, and great resistance to chemical attack. This optimization will eventually allow a-SiC:H to be used as an ideal insulation, passivation and protection layer for thin and biocompatible all-SiC neural interfaces.

Introduction

Neural interfaces allow for a direct connection between neural cells and external electronics, with many applications in neuroscience [1] and medicine [2]. A critical aspect of invasive neural interfaces is the biocompatibility as well as the ruggedness of the implant, which can affect the longevity of the devices and cause damage to the surrounding tissue. As neural interfacing technology has matured, devices with higher channel counts and smaller, more flexible electrodes have become increasingly desirable. This development comes with increasingly stringent material requirements, as the electrical passivation and chemical protection must also scale both in size and performance to maintain high-quality passivation at modern device scales.

Specifically, neural interface passivation must maintain high resistivity in a liquid environment even for film thicknesses on the order of several hundreds of nanometers. Additionally, the film must resist dissolution and remain pinhole free over a minimum of several months in physiological conditions, with a goal of extending the lifetime to multiple years. Typical neural interface passivation materials, such as SiO_2 [3] or parylene C [4], have extended the lifetimes of research-grade neural interfaces beyond a year, but remain fundamentally limited by the material response in-vivo as well as the minimum thickness required to achieve reliable long-term passivation..

PECVD a-SiC:H has previously been shown to be a robust, chemically-inert, and highly insulating coating material, making it an appealing material for passivation layers in neural interface applications [5-6]. However, it commonly results in high-stress films that are prone to delamination and device failure. Several studies have examined the optimization of PECVD process parameters towards minimizing the film stress by controlling the deposition temperature [7], RF power [8], precursor flow rates [9], and hydrogen incorporation [10]. Most studies use precursor gases of silane (SiH4) and methane (CH4), whereas Plasma-Therm Europe has developed a process using silane and ethylene (C_2H_4) for a-SiC deposition. This study must identify similarities and differences in the deposition behavior with this process gas mixture compared to the conventional methane processes more typical in literature before using any previous results to guide optimization.

An ideal a-SiC neural interface passivation layer must achieve low long-term stress to ensure devices remain stable while also achieving low resistivity for optimal passivation. Stress below 200 MPa (absolute) is desired along with resistivity above 1E12 Ω.cm to match films typically used for neural interfaces. Furthermore, a stoichiometric Si:C 1:1 composition is desirable for high chemical etch resistance [11].

This study seeks first to replicate existing deposition results from literature with Plasma-Therm's methylene process, giving special consideration for the parameters relevant to neural interfaces, and will pursue a broad characterization of the film properties in order to determine the influence of typical PECVD deposition parameters on the finished films with this process in order to improve the deposition quality of long-lasting, resistive passivating films.

Film Deposition

The films are deposited by Plasma-therm Europe by PECVD using a variety of process conditions. Silane (SiH4) and ethylene (C_2H_4) are used as precursor gases with an Ar carrier gas, on 2" Si wafers with a 100nm SiO_2 passivation layer is deposited immediately prior to a-SiC:H deposition. A baseline set of deposition conditions (sample 1) had previously been found to result in high reliability and adequate, but not state-of-art, performance, and was used as a starting point for optimization.

Table I. Process Parameters for Experimental Samples

#	Temperature [°C]	Power [W]	SiH_4 Flow [sccm]	C_2H_4 Flow [sccm]	H_2 Flow [sccm]	Ar Flow [sccm]	Pressure [mTorr]	Deposition Rate [nm/min]
1	300	220	50	87	0	600	1200	136.7
2	220	220	50	87	0	600	1200	142.8
3	150	220	50	87	0	600	1200	181.4
4	300	220	50	50	0	600	1200	173.6
5	300	220	33	58	0	400	1200	132.9
6	300	220	33	58	0	645	1200	114.2
7	300	220	50	87	0	600	800	125.7
8	300	150	50	87	0	600	1200	114.5
9	300	100	50	87	0	600	1200	89.7
10	300	220	50	87	300	300	1200	135.8
11	300	220	50	87	570	30	1200	143.2

Film Characterization

To fully characterize the films, a broad array of characterization techniques are used. The film composition and bonding is studied using Raman Spectroscopy [12], and the incorporation of hydrogen is studied using Fourier Transform Infrared Spectroscopy (FTIR) and extracted following a process from literature [13]. The film stress is determined by optical profilometry, measured from the curvature of the sample and calculated using the Stoney equation. The measurements were repeated multiple times after deposition to track the evolution of stress when exposed to the environment, with only the final, consistent value shown in Table II (all measurements are shown in Fig. 2). The refractive index is obtained from the Tauc-Lorentz model using optical ellipsometry. The full material characteristics of each layer of the samples are modelled, and regression is performed to minimize the difference between the data and model. The film resistivity is determined by depositing 500nm thick Al contacts on the surface of the films and measuring the resistance using a Keysight B1500A semiconductor device parameter analyzer.

Table II. Selected Results for Experimental Samples

#	Si/C ratio	Hydrogen content [%]	Refractive Index	Final Stress [MPa]	Stress change 33 days [MPa]	Resistivity [Ω.cm]
1	1.20	16	2.55	-327	-84	2.6E9
2	1.13	15	2.42	-322	-82	6.5E10
3	0.70	17	2.25	-210	-12	9.1E12
4	1.39	11	2.69	-271	-41	4.3E12
5	0.55	16	2.43	-327	-69	4.4E11
6	1.03	16	2.49	-421	-139	3.0E9
7	1.22	15	2.62	-454	-161	4.2E9
8	1.68	17	2.53	-591	-376	3.5E9
9	1.85	18	2.54	-529	-342	2.2E10
10	2.19	15	2.65	-569	-211	6.1E8
11	2.40	13	2.67	-561	-151	4.5E9

The composition, refractive index, and resistivity of these samples are within the expected bounds for these types of films, while the stress is slightly more compressive than desired.

Film Composition. Film composition correlates with the ratio of precursors as expected [14] (Fig. 1a), but is also affected strongly by the deposition temperature, total precursor flow, and RF power. The same relation between composition and power (Fig. 1b) has been reported in CH_4-precursor samples [8], and explained by the lower power reducing the ablative etching of Si-Si bonds due to reduced ion bombardment. Si content also decreases as the temperature increases, which may be explained by the increased temperature encouraging a more energetically-favorable 1:1 Si:C composition. The increase in Si content with total precursor flow is likely explained by the difference in reactivity of SiH_4 and C_2H_4, as the more-reactive SiH_4 is more likely to deposit in the shorter dwell times of the high-flow regime.

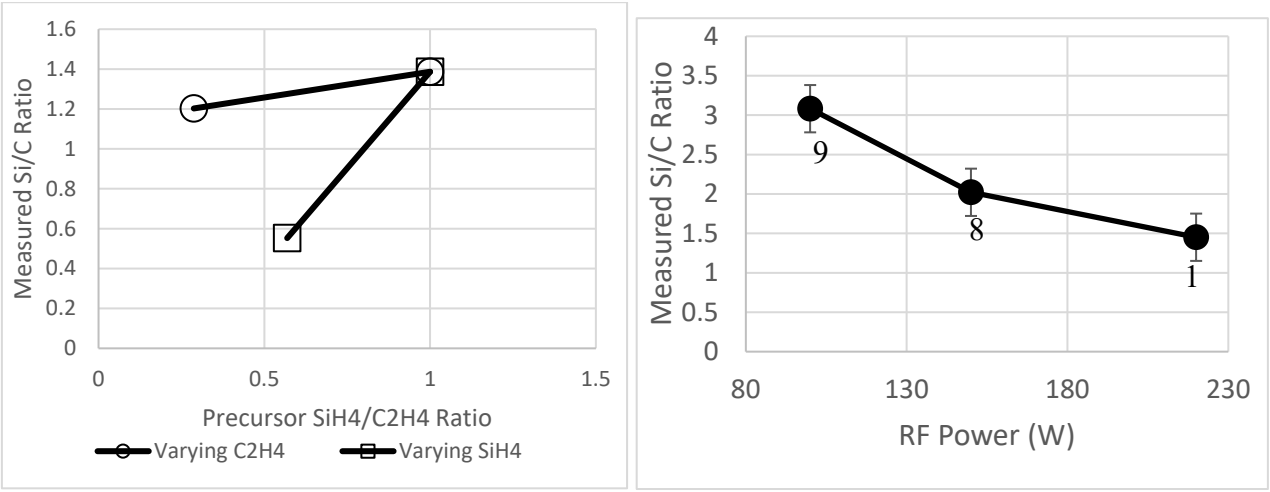

Fig. 1. Effect of input parameters on output film composition. a) Variation of film Si/C composition ratio as a function of precursor gas Si/C ratio. Under these conditions, varying SiH_4 has a much greater effect on the film composition than varying C_2H_4. b) Variation on Si/C ratio as a function of RF power.

The films' hydrogen content correlates most strongly with power and H_2 flow. Increasing the H_2 flow decreases the H content in the films (Fig. 2a) by selectively etching the weak C-H and Si-H bonds and increasing Si-C order [10]. Decreasing the RF power results in increased H content (Fig. 2b). Lower power is expected to result in decreased etching of terminating H-bonds, resulting in a more porous, lower-density film structure.

The refractive index of the films correlates with the composition of the films and density, where films with higher C content and lower density result in lower refractive indices. This is again consistent with typical results in literature using conventional precursors [15].

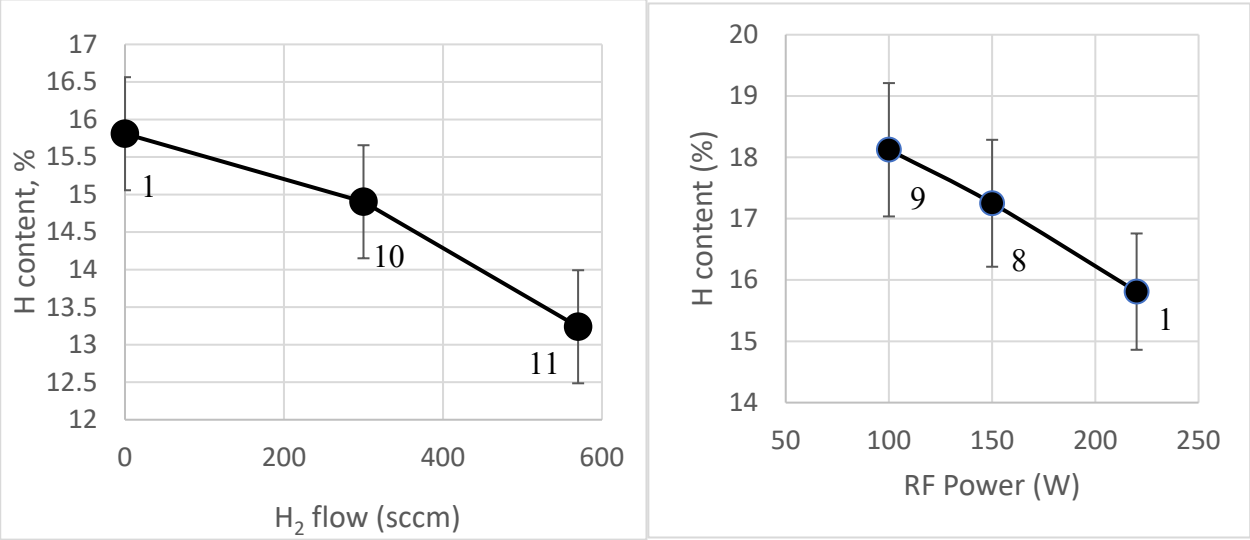

Fig. 2. Details of composition measurements. a) Decrease in H content as H_2 flow increases. b) Increase of H content as RF power decreases.

Film Stress. The stress measurements were repeated multiple times for each sample in order to track the time evolution of the stress for the exposed samples. All samples were stored under the same conditions and exposed to air at ambient temperature for the duration of the study. All samples showed an increase in stress over time, explained by the incorporation of moisture into the films, and consistent with previous results in CH_4 films [16].

The film stress was correlated with the deposition temperature, RF power, and H_2 flow (Fig. 3.). Decreasing the deposition temperature (samples 2 and 3) results in a more disordered film, which decreases the film stress consistently over the duration of the measurements. Decreasing the RF power (samples 8 and 9) likewise increases disorder but also increases porosity, explaining the low initial film stress, an effect also observed by [16] in films deposited by CH_4. The high porosity allows additional moisture intake over time, which dramatically increases the stress, seen as a dramatic change over the first two weeks of the film life. Adding H_2 flow (samples 10 and 11), which increases chemical ordering and passivates dangling bonds, also increases the film stress.

While none of the films achieved a stress below 200 MPa after exposure to the environment, the low temperature film achieves near-desired performance before further optimization.

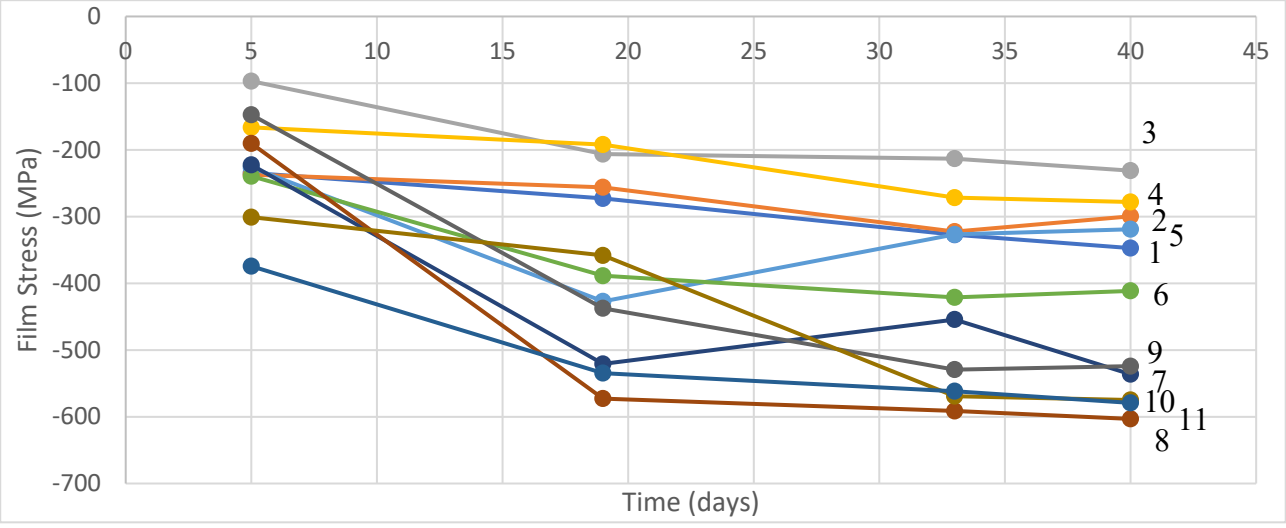

Fig. 3. Evolution in film stress as measured by optical profilometry over 40 days.

Resistivity. The film resistivity correlates most strongly with the deposition temperature, showing a dramatic increase in resistivity for lower temperatures (Fig. 4), consistent with reported results in the literature for CH_4 [17]. At the lowest temperature, the desired resistivity value is exceeded, demonstrating the potential of this a-SiC recipe for passivation. A smaller increase in resistivity was also observed as the RF power decreased. Both results together suggest that the increased disorder does not lead to defect sites for enhanced electron hopping. Higher temperature deposition is expected to increase the nanocrystallinity of the amorphous films, which is associated with lower resistivity.

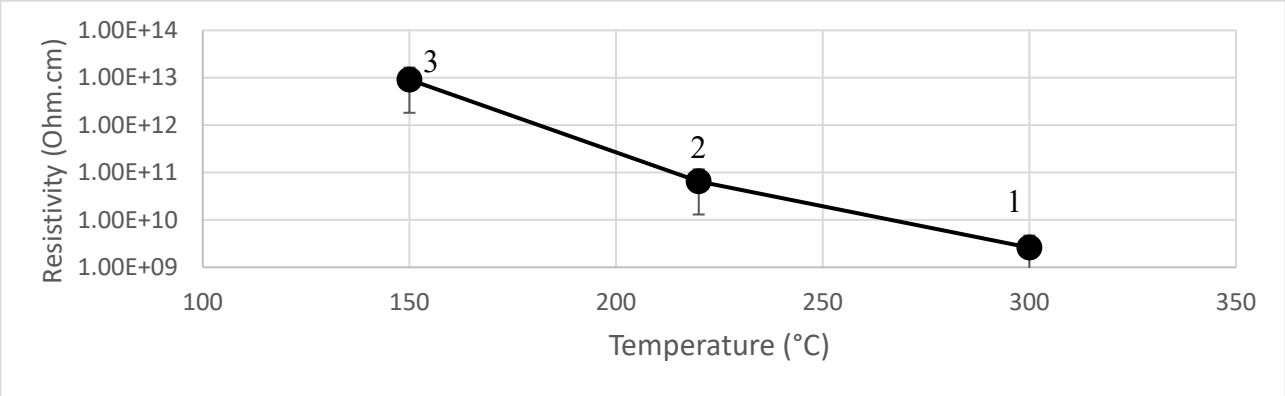

Fig.4. Change in film resistivity as a function of deposition temperature.

Summary

This study validates several similarities of PECVD deposition of a-SiC:H using an ethylene precursor compared to the more common methane precursor while identifying several other trends between input parameters and film properties. The film stress can be controlled by the RF power, deposition temperature, and hydrogen flow during deposition. The resistivity can be increased most effectively by lowering the deposition temperature. Lastly, the film composition can straightforwardly be controlled by changing the ratio of precursor gasses. By varying these parameters, films with properties near to state-of-the-art for neural interface passivation can be achieved.

While this initial study suggests that many of the known relations between deposition parameters and film properties identified previously in methane-precursor processes are also valid for the methylene-based process, the utility and reliability of these results is limited by the small sample sizes for each experiment. A Plackett-Burman Design of Experiment method could be used to more thoroughly identify the effects of each process parameter as well as to identify more complicated deposition properties where multiple input parameters interact nonlinearly, which requires further study.

Increased control over the film properties of PECVD a-SiC:H is critical not only for neural interface passivation, but broadly applicable to MEMS devices requiring a combination of mechanical strength, chemical resistance, and electrical or optical optimization.

This study examines the mechanical, compositional, and electrical properties of PECVD a-SiC:H as a function of a variety of deposition conditions. The film Si and C composition could be controlled by the ratio of precursor gasses, the total flow rate of precursors, the deposition temperature, and the RF power. Hydrogen content could be decreased by adding H_2 flow in the precursor mix, and increased by decreasing the RF power. Stress was minimized both as-deposited and after ambient exposure by lowering the deposition temperature. Furthermore, lower deposition temperatures also increased the film resistivity.

References

[1] N. Hatsopoulos, J. Donoghue. The Science of Neural Interface Systems. Annual review of neuroscience. 32 (2009) 249-66.

[2] N. H. Lovell, J. W. Morley, S. C. Chen, L. E. Hallum and G. J. Suaning, Biological–Machine Systems Integration: Engineering the Neural Interface. Proceedings of the IEEE, vol. 98 (2010) 3, 418-431.

[3] C.H. Chiang, S.M. Won, A.L. Orsborn, K.J. Yu, M. Trumpis, G. Bent, C. Wang, Y. Xue, S. Min, V. Woods, C. Yu, B.H. Kim, S.B. Kim, R. Huq, J. Li, K.J. Seo, F. Vitale, A. Richardson, H. Fang, Y. Huang, K. Shepard, B. Pesaran, J.A. Rogers, J. Viventi. Development of a neural interface for high-definition, long-term recording in rodents and nonhuman primates. Sci Transl Med. 2020 Apr 8;12(538):eaay4682. doi: 10.1126/scitranslmed.aay4682. PMID: 32269166; PMCID: PMC7478122.

[4] J.M. Hsu, L. Rieth, R.A. Normann, P. Tathireddy, F. Solzbacher. Encapsulation of an integrated neural interface device with Parylene C. IEEE Trans Biomed Eng. 2009 Jan;56(1):23-9. doi: 10.1109/TBME.2008.2002155. PMID: 19224715.

[5] F. Deku, Y. Cohen, A. Joshi-Imre, A. Kanneganti, T.J. Gardner, S.F. Cogan. Amorphous silicon carbide ultramicroelectrode arrays for neural stimulation and recording. J Neural Eng. (2018) Feb; 15(1):016007.

[6] C. Feng & C. Frewin & M. R. Tanjil & R. Everly & J. Bieber & A. Kumar & M.C. Wang & S.E. Saddow. A Flexible a-SiC-Based Neural Interface Utilizing Pyrolyzed-Photoresist Film (C) Active Sites. Micromachines. 12. (2021). 10.3390/mi12070821.

[7] M.Avram, A.Avram, A. Bragaru, B.Chen, D. Poenar, C. Iliescu. Low stress PECVD amorphous silicon carbide for MEMS applications. Semic. Conf. CAS 2010 Int. (2010). 01. 239-242.

[8] S. Kwon, Y. Park, W. Ban, C. Youn, S. Lee, J. Yang, D. Jung, T. Choi. Effect of plasma power on properties of hydrogenated amorphous silicon carbide hardmask films deposited by PECVD. Vacuum (2020) Apr;174.

[9] Y. Inoue, S. Nakashima, A. Mitsuishi, S. Tabata, S. Tsuboi. “Raman spectra of amorphous SiC.” *Solid State Communications* 48 (1983): 1071-1075.

[10] J.M. Hsu, P. Tathireddy, L. Rieth, A.R. Normann, F. Solzbacher. Characterization of a-SiC(x):H thin films as an encapsulation material for integrated silicon based neural interface devices. Thin Solid Films. (2007) Nov 1;516(1):34-41.

[11] Diaz-Botia. “Silicon carbide technologies for interfacing with the nervous system” PhD thesis, University of California, Berkeley. (2017).

[12] Y. Inoue, S. Nakashima, A. Mitsuishi, S. Tabata, S. Tsuboi, Raman spectra of amorphous SiC, Solid State Communications, Volume 48, Issue 12, 1983, Pages 1071-1075, ISSN 0038-1098, https://doi.org/10.1016/0038-1098(83)90834-7.

[13] H. Wieder, M. Cardona, C.R. Guarnieri. Vibrational Spectrum of Hydrogenated Amorphous Si-C Films. Phys. Stat. Sol. (b) (1979) 92, 99

[14] W. Daves, A. Krauß, N. Behnel, V. Häublein, A. Bauer, L. Frey. Amorphous silicon carbide thin films (a-SiC:H) deposited by plasma-enhanced chemical vapor deposition as protective coatings for harsh environment applications. Thin Solid Films. 519. (2011). 5892-5898.

[15] S. King, J. Bielefeld, G. Xu, W. Lanford, Y. Matsuda, R. Dauskardt, N. Kim, D. Hondongwa, L. Olasov, B. Daly, G. Stan, M. Liu, D. Dutta, D. Gidley. Influence of network bond percolation on the thermal, mechanical, electrical and optical properties of high and low-k a-SiC:H thin films. Journal of Non-Crystalline Solids. 379. (2013). 67. 10.1016/j.jnoncrysol.2013.07.028.

[16] F. Deku, S. Mohammed, A. Joshi-Imre, J. Maeng, V. Danda, T.J. Gardner, S.F. Cogan. Effect of oxidation on intrinsic residual stress in amorphous silicon carbide films. J Biomed Mater Res B Part B. (2018). 2018:9999:9999:1–8.

[17] Stefan Janz, “Amorphous Silicon Carbide for Photovoltaic Applications”, PhD Dissertation Un.Konstanz Germany, 2006